

# An Automated Scheme to Determine Design Parameters for a Recoverable Re-entry Vehicle

W.E. Williamson\*

Sandia Laboratories, Albuquerque, N.Mex.

The NRV (nosetip recovery vehicle) program is designed to recover the nose section from a sphere cone re-entry vehicle after it has flown a near-ICBM re-entry trajectory. Both mass jettison and parachutes are used to reduce the velocity of the RV near the end of the trajectory to a sufficiently low level that the vehicle may land intact. The design problem of determining mass jettison time and parachute deployment time in order to insure that the vehicle does land intact is considered in this paper. The problem is formulated as a minimum-maximum optimization problem where the design parameters are to be selected to minimize the maximum possible deviation in the design criteria because of uncertainties in the system. The results of the study indicate that the optimal choice of the design parameters ensures that the maximum deviation in the design criteria is within acceptable bounds. This analytically insures the feasibility of recovery for NRV.

## Nomenclature

$a_0, \dots, a_q$	= parameters in polynomial representation of $C_A$
$C_A$	= axial force coefficient
$C_{A_{\min}}$	= minimum value of $C_A$ for specified values of $M$ and $R_e$
$C_{A_{\max}}$	= maximum value of $C_A$ for specified values of $M$ and $R_e$
$C_D$	= drag coefficient
$d$	= base diameter of re-entry vehicle
$D$	= drag force
$g$	= gravitational acceleration
$G$	= performance index
$h$	= altitude
$L$	= length of vehicle
$m$	= mass of vehicle
$M$	= Mach number
$p$	= polynomial representation of $C_A$
$q'$	= dynamic pressure
$q'_d$	= desired value of dynamic pressure at chute deployment
$q'_{\max}$	= maximum dynamic pressure at chute deployment
$q'_{\min}$	= minimum dynamic pressure at chute deployment
$R_e$	= Reynolds number per unit length
$r_n$	= nose radius of re-entry vehicle
$S$	= reference area of re-entry vehicle
$t$	= independent variable, time
$t_{mdp}$	= time at maximum dynamic pressure
$t_{sep}$	= vehicle separation time
$t_{cd}$	= vehicle chute deployment time
$V$	= velocity of vehicle
$W$	= weight of vehicle
$\theta$	= vehicle cone half-angle
$\gamma$	= vehicle flight-path angle

## Subscripts

0 = evaluated at initial time

Presented at the AIAA 3rd Atmospheric Flight Mechanics Conference, Arlington, Texas, June 7-9, 1976 (in bound volume of Conference papers, no paper number); submitted June 24, 1976; revision received April 15, 1977.

Index categories: Spacecraft Navigation, Guidance, and Flight-Path Control; Entry Vehicle Mission Studies and Flight Mechanics.

\*Member of Technical Staff, Aeroballistic Projects Division. Associate Fellow AIAA.

## Introduction

AN important phase of re-entry vehicle (RV) research involves the testing of new nosetip materials. In most cases, the performance of the material is related directly to the nosetip shape recession history during re-entry. Although some quantitative statements can be made about the nosetip recession after a flight test, the actual nosetip shape recession history is extremely difficult to compute. Thus, information concerning the final nosetip shape after re-entry would be extremely useful for evaluating nosetip materials.

The purpose of the NRV (nosetip recovery vehicle) program is to recover the nosetip of a sphere cone re-entry vehicle after a typical ICBM re-entry trajectory and hence to allow the final nosetip shape to be observed. The concept used to attempt to recover the nosetip consists of substantially reducing the ballistic coefficient of the vehicle near the end of the trajectory. This is accomplished by segmenting the vehicle. The last section of the cone, including more than half of the weight of the RV, is jettisoned near the end of the trajectory. This reduces the ballistic coefficient of the RV substantially and causes the nose segment of the vehicle to decelerate very rapidly. If the system is designed properly, it is possible to reduce the velocity of the nose segment to a sufficiently low level that a parachute may be deployed by the RV. This allows the velocity of the RV to be reduced further to a level that will allow the vehicle to land intact. Note that the segmentation should occur after peak dynamic pressure, so that the nosetip will have experienced the desired heating rates for the original vehicle flying a near-ICBM re-entry trajectory. The purpose of this paper is to describe a technique that may be used to compute segmentation and parachute deployment times that insure the safe recovery of the vehicle in spite of uncertainties in the re-entry trajectory.

Table 1 Constants associated with NRV and its re-entry trajectory

Variable	NRV	NRV after mass jettison
$S$	0.775 ft <sup>2</sup>	0.61978 ft <sup>2</sup>
$d$	1.0 ft	0.8883 ft
$W$	102.9 lb	40.8 lb
$\theta$	6°	6°
$r_n$	1.25 in.	1.25 in.
$L$	3.833 ft	3.302 ft
$h_0$	100,000 ft	...
$V_0$	19,104 fps	...

### Design Problem

The preliminary design phase of the NRV program resulted in the development of the vehicle described in Ref. 1. Its geometry and mass properties are shown in Table 1. The only design variables considered in this paper which could be selected to insure a safe recovery of NRV were the vehicle segmentation time, the parachute deployment time, and the initial flight-path angle. Values for these variables should be selected in order to insure that the RV experiences a typical heating environment from a near-ICBM re-entry trajectory and that the nose segment of the vehicle lands intact. It should be noted, however, that the design scheme easily could have been extended to determine properties of the vehicle such as bluntness ratio or percentage of the mass to be jettisoned. These variables easily could be treated as additional parameters, and, since their relationship to the design criteria would be established by the dynamic model, values that extremize the design criteria could be computed.

The critical design criterion, in order to meet the objectives just stated, is that the dynamic pressure and altitude at chute deployment both must be within acceptable bounds. If an attempt is made to open the chute too early, the dynamic pressure will be too high, and the chute will be destroyed when it is opened. If the timer setting is too late, the dynamic pressure will be too low, and the parachute will not open properly. For NRV, acceptable bounds for the dynamic pressure are approximately 800 to 2400 psf. If the dynamic pressure is between these two numbers, then the parachute should open properly. Even if the dynamic pressure at chute deployment is within the acceptable bounds, it also is necessary for the altitude to be sufficiently high that the RV has time to decelerate before hitting the ground. Thus the chute must be deployed by 1500 ft or higher above the ground. This will allow enough time before the vehicle reaches the ground so that the chute can decrease the velocity substantially and allow the vehicle to be recovered intact.

For NRV, the segmentation time was specified by a timer actuated when the axial acceleration reached a specified level. The parachute was deployed by a timer that was initiated at segmentation. Thus the design problem consisted of determining these two timer settings and the initial flight-path angle to insure that chute deployment occurred at an acceptable value of dynamic pressure and altitude.

The design problem just described could be solved easily if the aerodynamic coefficients of the vehicle, the atmospheric properties, and the initial re-entry conditions were known exactly. It would be necessary to compute the RV's trajectory for several initial flight-path angles while varying the segmentation time for each angle. It should be easy to select

an initial flight-path angle and segmentation time that produce the desired dynamic pressure for chute deployment after segmentation. If the corresponding altitude is sufficiently high, then the problem has been solved. From the results shown later, the altitude at chute deployment is sufficiently high for most reasonable choices of the design parameters. Thus the problem could have been solved easily in this manner.

Unfortunately the atmospheric properties, aerodynamic coefficients, and initial re-entry conditions are not known exactly. The fact that these quantities are not known exactly means that the exact dynamic pressure at chute deployment cannot be computed. It is thus necessary to determine how the uncertainty in these quantities affects the dynamic pressure at chute deployment and then to select the timer settings to minimize the effect.

A preliminary investigation of the effects of uncertainties in the quantities just described indicates that a lack of knowledge of  $C_A$  causes the largest changes in dynamic pressure at chute deployment. Thus, whether predictions for  $C_A$  are higher or lower than the actual value substantially alters the dynamic pressure at chute deployment.

Values of  $C_A$  are a function of angle of attack, Mach number, Reynolds number, the shape of the RV, and whether the flowfield is laminar or turbulent. Thus,  $C_A$  changes considerably along the trajectory. Instead of having changes in one number, such as the initial velocity, it is possible to have values of  $C_A$  which are both higher and lower than nominal values at different points along the trajectory. Thus, the effect of uncertainties in a  $C_A$  history which is a function of the trajectory must be determined.

This problem is solved by first defining a nominal  $C_A$  history for the RV. Error bounds on  $C_A$  all along the trajectory then are computed. It then is possible to compute  $C_A$  histories within these boundaries which generate the highest value for the dynamic pressure or the lowest value for the dynamic pressure at chute deployment. Note that this is a standard calculus of variations or optimal control problem. Standard numerical techniques can be used to define the  $C_A$  history that produces minimum or maximum dynamic pressure at chute deployment.<sup>3</sup> After these are computed, it then is possible to select the timer settings to minimize the difference between the minimum and maximum dynamic pressure at chute deployment and some desired value. This is a standard parameter optimization problem.<sup>3</sup> Thus, the design problem can be formulated as a minimum-maximum problem where the timer settings and the initial flight-path angle should be selected to minimize the maximum dynamic pressure deviation from the desired value. In this case, the two optimization problems are coupled. Thus, the solution of one of the problems depends on the solution for the other. Minimum-maximum problems such as the one just described are, in general, extremely difficult optimization problems. Fortunately, in this case, the minimization and the maximization may be done separately. This is described later.

### Bounds on Axial Force Coefficient

In order to estimate the effect of the uncertainty in  $C_A$  on the trajectory, both the predicted values for  $C_A$  and the error bounds must be obtained. The predicted axial force coefficient history was computed using the hypersonic aerodynamic computer program (HABS)<sup>2</sup> and is shown in Fig. 1. The error bounds shown in Fig. 1 are computed by comparing predictions of  $C_A$  using HABS with actual values obtained from flight tests of seven similar vehicles. Thus, the error bounds shown in Fig. 1 reflect the ability of the computer program to predict  $C_A$  for seven previous flight tests. The independent variable chosen for the comparisons was  $M/\sqrt{R_e}$ , since this reflects the importance of the Mach number and Reynolds number during different flight regimes. The effect of early or late transition on  $C_A$  is shown in Fig. 1. The effect was computed by assuming that transition occurred at

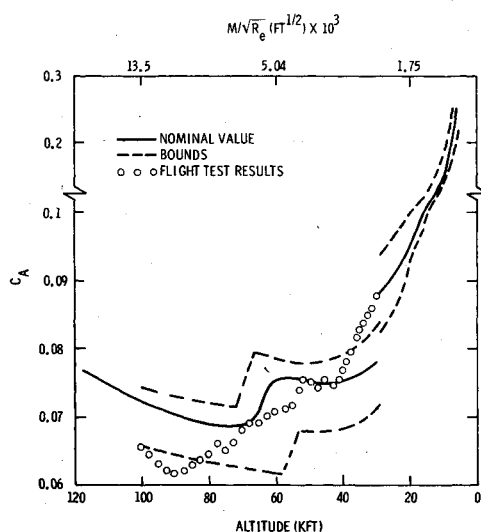


Fig. 1 Nominal value and predicted bounds for  $C_A$  for NRV.

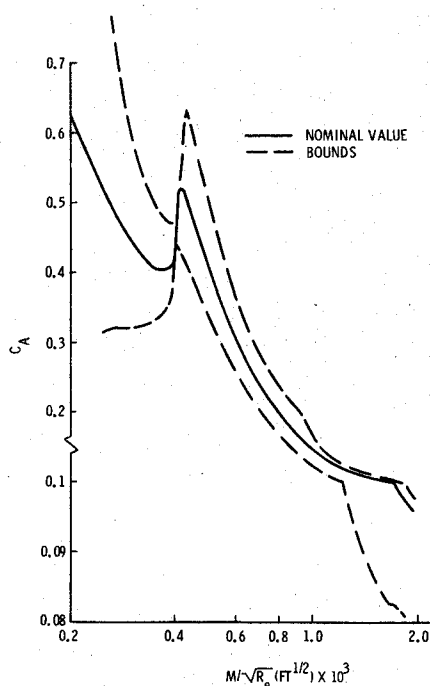


Fig. 2 Nominal value and predicted bounds for  $C_A$  after vehicle separation.

Table 2 Values of parameters for minimum or maximum dynamic pressure at chute deployment

Maximum dynamic pressure	
$a_0 = 1.57$	$a_3 = 0.00$
$a_1 = 0.00$	$a_4 = 0.00$
$a_2 = 0.00$	$a_5 = 0.00$
Minimum dynamic pressure	
$a_0 = 0.00$	$a_3 = 1.57$
$a_1 = 0.00$	$a_4 = 0.00$
$a_2 = 0.00$	$a_5 = 0.00$

72.3 kft for early transition and at 58.7 kft for late transition instead of the predicted altitude of 65.5 kft.<sup>7</sup> This allowed bounds on  $C_A$ , assuming early or late transition to be computed.

The Mach number for NRV will not be in the hypersonic range near the end of the flight. Thus, values for  $C_A$  computed using HABS are not realistic after vehicle separation. An alternate effort to predict  $C_A$  and its error bounds was completed in Ref. 8. In this approach, techniques much more sophisticated than are used in HABS were used to predict  $C_A$ . Estimates of the bounds on parameters in the schemes, used to compute viscous and inviscid components of the drag, were used to compute error bounds on  $C_A$ . The nominal values and bounds for  $C_A$  after the vehicles are separated are shown in Fig. 2. Since this approach should give better estimates of  $C_A$  at the lower Mach numbers, the results of Fig. 2 are used to provide the nominal value of  $C_A$  and its bounds after separation.

### Optimization Studies

After bounds for  $C_A$  have been determined, it is possible to compute trajectories with maximum or minimum dynamic pressure for specified values of the timer settings and initial flight-path angle. The only restriction on these trajectories is that the axial force coefficient must lie within the specified bounds. These trajectories thus reflect the worst cases that could arise from an inability to predict  $C_A$  accurately. The problem is to determine the  $C_A$  history within the bounds

which does generate the worst values for dynamic pressure at chute deployment.

This problem may be formulated as a standard optimal control (calculus of variations) problem with a bounded control variable. The dynamics can be modeled well using the two-dimensional point mass equations for a flat Earth. Thus, the state equations are

$$\dot{h} = V \sin \gamma \quad \dot{V} = -D/m - g \sin \gamma \quad \dot{\gamma} = -g \cos \gamma / V \quad (1)$$

The state variables are  $h$ ,  $V$ , and  $\gamma$ , and the control variable is  $C_D$  or, for small angle of attack,  $C_A$ . The simple state model is used, since it represents the important features of re-entry while allowing the rapid computation of trajectories, which is desirable for an optimization program that numerically computes a large number of re-entry trajectories.

A large number of numerical methods could be used to solve this optimal control problem.<sup>3</sup> Since the state equations are linear in the control variable, however, a large number of the standard numerical optimization schemes cannot compute solutions to this problem efficiently. A class of methods which does seem to work well is the parameterization schemes described in Refs. 4 and 5. By using numerical partial derivatives, these schemes require only that a numerically computable functional relationship exist between the quantity to be optimized, dynamic pressure, and the parameters to be computed, the  $a$  vector. This is provided by the differential equations (1). Thus, the calculus of variations problem is reduced to a parameter optimization problem by assuming that the optimal  $C_A$  history can be approximated by

$$C_A = (C_{A_{\max}} - C_{A_{\min}}) \sin^2 p + C_{A_{\min}} \quad (2)$$

where  $p$  is a polynomial in time. Thus, in general,

$$p = a_0 + a_1 t + a_2 t^2 + \dots + a_q t^q \quad (3)$$

where the  $a$ 's are to be determined. The value of  $q$  is specified and is chosen to be sufficiently large so that a fairly general control shape may be represented. The minimum and maximum values of  $C_A$  are functions of  $M/\sqrt{R_e}$ . The form chosen for  $C_A$  insures that its value is between  $C_{A_{\max}}$  and  $C_{A_{\min}}$  all along the trajectory. Once the control is parameterized, it is necessary to determine the constants in  $p$ , the  $a$ 's, rather than the entire control history  $C_A$ . This substantially reduces the computational difficulties associated with the problem.

Since there is a discontinuity in the  $C_A$  history at separation, different polynomials were used over the first and second segments. Over the first segment in time,

$$p = a_0 + a_1 t + a_2 t^2 \quad (4)$$

and, after the vehicle is separated,

$$p = a_3 + a_4 t + a_5 t^2 \quad (5)$$

Thus six values of the parameters characterize the shape of the  $C_A$  history both before and after separation. The polynomial  $p$  was chosen to be a parabola over each segment, since this allows reasonable changes in the  $C_A$  history without introducing too many coefficients. Also, the actual value of  $C_A$  is not expected to oscillate rapidly about the predicted value. Hence a parabola should represent reasonable uncertainties in  $C_A$ .

Re-entry for NRV is assumed to begin at an altitude of 300 kft, with a velocity of 19,080.5 fps. Changes in  $C_A$  do not begin to alter the trajectory substantially until the altitude is below 100 kft. In order to decrease the computing time, all trajectories were computed from 100 kft. The velocity used at 100 kft is shown in Table 1 and was computed by integrating the nominal  $C_A$  history from 300 to 100 kft using a six-degree-

of-freedom computer program. The 1962 Standard Atmosphere was used to compute the atmospheric density.

The first step in solving the design problem was to select representative timer settings and an initial flight-path angle for NRV. The optimization scheme in Ref. 6 was then used in exactly the same manner that the Davidson scheme is used in Ref. 5 to find the values of the  $a$  vector which generate maximum or minimum dynamic pressure at chute deployment.

The control history for the solution to both of these problems was found to be entirely on the boundaries. Maximum dynamic pressure was obtained using the upper boundary for  $C_A$  before vehicle segmentation and the lower boundary after vehicle segmentation. Minimum dynamic pressure was obtained using the lower boundary before vehicle segmentation and the upper boundary after vehicle segmentation. The results for the parameters are shown in Table 2.

These results were not expected. It was anticipated that the largest dynamic pressure at  $t_{cd}$  would be obtained when  $C_A$  is on the lower boundary for the entire trajectory, and the smallest dynamic pressure at  $t_{cd}$  would occur when  $C_A$  is on the upper boundary. Intuition in this case tends to be based on simple solutions such as those shown by Allen and Eggers.<sup>9</sup> Reference 9, however, assumes that  $C_A$  is constant and uses altitude as the independent variable. In this case, dynamic pressure does increase as the ballistic coefficient ( $W/SC_D$ ) increases. Thus, as  $C_A$  decreases, dynamic pressure should increase at corresponding values of altitude. In this study  $C_A$  is not constant, all dynamic pressure comparisons are at fixed time intervals, not altitude intervals, and the separation process occurs. This causes the results obtained here to differ from expected results based on simple solutions such as those shown in Ref. 9.

Plots of the trajectories for the optimal timer settings computed later are shown in Figs. 3 and 4. The results in Fig. 3 are computed by using  $C_{A_{max}}$  before separation and  $C_{A_{min}}$  after separation. Results shown in Fig. 4 use  $C_{A_{min}}$  before separation and  $C_{A_{max}}$  after separation. The peak dynamic pressure is higher for the trajectory shown in Fig. 4 than for the one shown in Fig. 3. This is expected, since that trajectory was computed using the smallest value of  $C_A$  before separation. This causes the higher peak value of dynamic pressure, as Ref. 9 would predict. When  $C_A$  jumps to the maximum value after separation, this substantially increases the axial acceleration, resulting in a large dynamic pressure slope change. Thus dynamic pressure begins to drop much more rapidly than it would have if  $C_{A_{min}}$  had been used after separation. This causes the dynamic pressure in Fig. 4 to drop below that in Fig. 3, provided that the time interval between separation and chute deployment is sufficiently long.

The trajectory shown in Fig. 3 is generated by using the maximum value of  $C_A$  before separation. This results in a minimal value of peak dynamic pressure. By switching to the minimum  $C_A$  history, this produces a smaller dynamic pressure slope after separation than is seen in Fig. 4, which

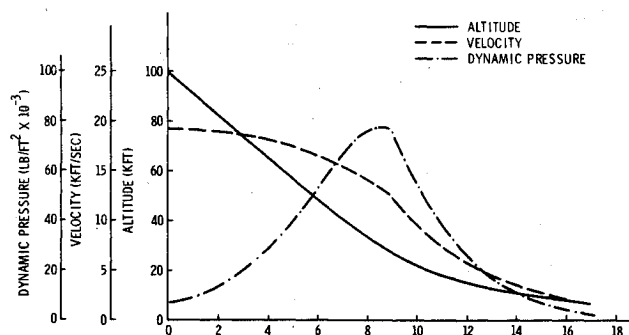


Fig. 3 Trajectory for NRV using  $C_A$  history that causes dynamic pressure to be a maximum at chute deployment.

allows the two curves to cross. The key element seems to be the time between separation and chute deployment. If it is sufficiently long, the results are as just described. It also is obvious that, if the time is sufficiently short, the boundary jump would not occur. This short time interval problem was not considered here, and only results of the type just described and the oscillatory solutions described later were computed.

As a check on the results, the dynamic pressure also was computed using  $C_{A_{min}}$  for both vehicles and  $C_{A_{max}}$  for both vehicles. The timer setting used for the comparisons are the optimal values shown in Table 3. Using  $C_{A_{min}}$  for the entire trajectory resulted in a dynamic pressure at chute deployment of 1920 psf, and using  $C_{A_{max}}$  for the entire trajectory resulted in a dynamic pressure at chute deployment of 1060 psf. Thus the values of  $q'$  computed using these  $C_A$  histories are between the minimum and maximum values, as they should be.

This optimization problem was solved for several different timer settings and initial flight-path angles, and in all cases the solutions described previously still were computed as optimal solutions. For the results shown in Table 3, for example, the flight-path angle can be varied at least between  $-25^\circ$  and  $-30^\circ$ , and  $t_{sep}$  can be increased to 3.0 sec, and the solutions described previously still are computed as optimal solutions. It should be noted that, as the sensitivity of the optimal control solution to the design parameters was being investigated, additional extremal  $C_A$  histories were obtained. Thus the solution to the problem appears to have more than one local extremal. In all cases, the additional extremals exhibited oscillatory behavior for the first vehicle and the same boundary segments as described earlier for the second vehicle.

These solutions did vary considerably as the parameters were changed, and no general trends were observed. The oscillatory nature of these solutions suggests the possibility that rapidly oscillating solutions, chattering, might be local extremal solutions. These solutions were not considered further, since the actual drag coefficient history is not expected to oscillate between the maximum and the minimum  $C_A$  histories. Also, the performance index for these solutions was within 7% of the values shown for the boundary segment solutions. Thus very little, if anything, would be gained by iterating toward a final solution with these control histories, whereas a much larger amount of computer time would be required, since the design problem and optimal control problem could not be separated. The local extremal solutions, consisting of the boundary segments described earlier, are the optimal solutions used in all of the work described here.

It thus can be concluded that, for reasonably small changes in timer settings and initial flight-path angle, the optimal solution consisting of the boundary segments is still an extremal solution. Thus, maximum dynamic pressure at chute deployment occurs if the actual value of  $C_A$  is as large as possible over the first segments and as small as possible over the second segment, irregardless of small changes in the

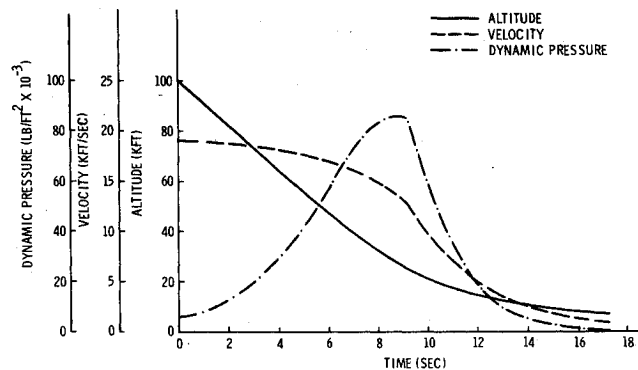


Fig. 4 Trajectory for NRV using  $C_A$  history that causes dynamic pressure to be a minimum at chute deployment.

Table 3 Results of optimization study

$\gamma_0$	$= -27.55^\circ$
$t_{sep}$	$= 2.5$ sec after $A_x = 35 g$
$t_{cd}$	$= 8.14$ sec after separation
$q'_{max}$	$= 2460$ psf
$q'_{min}$	$= 730$ psf

design parameters. The  $C_A$  history that causes a minimum value of dynamic pressure at  $t_{cd}$  also is independent of the design parameters. This allows the minimum-maximum problem to be divided into two problems. The first, solved previously, defines the  $C_A$  history that produces minimum and maximum values for dynamic pressure at  $t_{cd}$ . Once these are known, it is possible to find the design parameters that minimize the deviation of these values from a desired value. This is done below.

In order to determine  $t_{sep}$ ,  $t_{cd}$ , and  $\gamma_0$ , a minimization problem is formulated. The performance index is written as

$$G = (q'_{max} - q'_d)^2 + (q'_{min} - q'_d)^2$$

where  $q'_{max}$  is the maximum value of the dynamic pressure at  $t_{cd}$ , and  $q'_{min}$  is the minimum value of the dynamic pressure at  $t_{cd}$ . Both are determined by integrating Eq. (1) using the appropriate  $C_A$  history. They are both functions of  $t_{sep}$ ,  $t_{cd}$ , and  $\gamma_0$  through the numerical solution of the differential equations. The problem is to determine these three design variables so that  $G$  is a minimum.

The optimization was done again using the SRVM method described in Ref. 5. The initial flight-path angle was constrained to be between  $-25^\circ$  and  $-30^\circ$ . The separation time was constrained to occur after peak dynamic pressure, and the chute deployment time was constrained to occur after separation. A value of  $q'_d = 2000$  psf was used.

The results of the minimization problem are shown in Table 3. The trajectories, which produce minimum and maximum values of  $q'$  at  $t_{cd}$ , are shown in Figs. 3 and 4. The separation time  $t_{sep}$  was on the boundary. Thus separation should occur as soon as allowable after peak dynamic pressure. The initial flight-path angle was not on a boundary, as might have been expected. Both  $q'_{max}$  and  $q'_{min}$  are relatively close to 2000 psf and are within acceptable limits for parachute deployment. The altitude at chute deployment for both cases was approximately 6000 ft. This is well above the minimum altitude of 1500 ft. Thus, the minimum altitude constraint never was required.

After the optimal timer settings and initial flight-path angle were obtained, the problem of determining the  $C_A$  history that produced the largest and smallest values of  $q'$  at chute deployment was resolved using the optimal values for  $t_{cd}$ ,  $t_{sep}$ , and  $\gamma_0$ . The results did not change. This again justified separating the minimum-maximum problem into two problems.

Thus the original minimum-maximum problem was solved by first determining the axial force coefficient history that resulted in minimum or maximum dynamic pressure at chute deployment. Design parameters then were determined to insure that the extremal values of dynamic pressure were within acceptable limits.

## Summary and Conclusions

The problem of designing separation and parachute deployment times and the initial flight-path angle to recover the nose of a sphere cone re-entry vehicle has been discussed. The problem was formulated as a minimum-maximum design problem. It was shown that the problem could be broken into two separate problems. The first involves determining the axial force coefficient history that results in minimum or maximum values of dynamic pressure at chute deployment. The results of this study indicate that maximum dynamic pressure at chute deployment is obtained when the actual value of  $C_A$  is as large as possible within the specified bounds before vehicle separation and as small as possible after vehicle separation. Minimum dynamic pressure at chute deployment is obtained when  $C_A$  is as small as possible before vehicle separation and as large as possible after separation. The design parameters then are determined to keep the maximum and the minimum values of the dynamic pressure as near as possible to a desired value for the dynamic pressure. The final results indicate that the worst-case values for dynamic pressure and altitude are within acceptable limits for the NRV program.

The values of  $C_A$  obtained from the NRV flight test are shown in Fig. 1. The accuracy of the instrumentation was not adequate to permit values of  $C_A$  to be computed after separation. As can be seen from Fig. 1, the values of  $C_A$  are generally inside the bounds. The results of the dynamic analysis in Ref. 10 indicate that the vehicle flew very near the predicted nominal trajectory. Thus the timers were set at values that allowed the safe recovery of the vehicle in spite of the uncertainty in  $C_A$ .

## Acknowledgment

This work was supported by the U.S. Energy Research and Development Administration.

## References

- English, E.A., "Nosetip Recovery Vehicle Postflight Development Report," Sandia Labs., Rept. SAND 75-8059, Livermore, Calif., Jan. 1976.
- Gentry, A.E., "Hypersonic Arbitrary Body Aerodynamic Computer Program, Mark III Version," Douglas, Rept. DAC 61552, April 1962.
- Bryson, A.E. and Ho, Y.C., *Applied Optimal Control*, Blaisdell Publishing Co., Waltham, Mass., 1969.
- Williamson, W.E., "The Use of Polynomial Approximations to Calculate Suboptimal Controls," *AIAA Journal*, Vol. 9, Nov. 1971, pp. 2271-2273.
- Kamm, J.L. and Johnson, I.L., "Optimal Shuttle Trajectory-Vehicle Design Using Parameter Optimization," AIAA Paper 71-329, Ft. Lauderdale, Fla., 1971.
- Williamson, W.E., "Square-Root Variable Metric Method for Function Minimization," *AIAA Journal*, Vol. 13, Jan. 1975, pp. 107-109.
- Bulmer, B., private communication of unpublished material, Sandia Labs., May 1975.
- McBride, D., private communication of unpublished material, Sandia Labs., May 1975.
- Allen, H.J. and Eggers, A.E., "A Study of the Motion and Aerodynamic Heating of Ballistic Missiles Entering the Earth's Atmosphere at High Supersonic Speeds," NACA Rept. 1381, 1958.
- Hanrahan, J., "Nosetip Recovery Vehicle (NRV) Trajectory and Dynamics Data Package," Xonics, Inc., DCD 319, Dec. 1975.